COMPARISON OF STRENGTH PROPERTIES OF NORMOTENSIVE AND HYPERTENSIVE RAT PULMONARY ARTERIES

E.S. Drexler, C.N. McCowan, J.E. Wright, A.J. Slifka, D.D. Ivy*, and R. Shandas*
NIST, Materials Reliability Division, 325 Broadway, Boulder, CO 80305
*The Children's Hospital of Denver, 1056 E. 19th Ave., Denver, CO 80218

ABSTRACT

A series of tests were conducted to quantify the difference in the mechanical properties of normo- and hypertensive pulmonary arteries. A bubble-test design was employed to measure the biaxial properties of a segment of artery. The test results compare the properties at multiple orientations of the trunk, right, and left pulmonary arteries from normal (Control) and monocrotaline-treated male Long-Evans wild rats that ranged in age from 8 to 17 weeks old, along with some preliminary results from hypoxic Long-Evans knock-out rats. Data show little difference between the stress-strain relationship of the control pulmonary arteries and that of the monocrotaline-treated pulmonary arteries. However, the preliminary results from the hypoxic pulmonary arteries show that the arterial material strains less before the onset of strain-stiffening behavior. The longitudinal orientation exhibits strain stiffening at lower strains than does the circumferential orientation. The differences between the left and right main arteries are minor. The trunk consistently demonstrates less stiffening in the region of larger strains for all conditions.

INTRODUCTION

A rat model is a common first step in understanding diseases, such as pulmonary hypertension, in humans [1-6]. In this study, we are using (wild) Long-Evans rats to establish a baseline of mechanical properties for the pulmonary trunk and main arteries under normal conditions and comparing that to the mechanical properties of the proximal pulmonary arteries from monocrotaline-treated (MCT) Long-Evans rats and hypoxic Long-Evans rats with the endothelin-B receptor disabled (knock-out). Disabling the endothelin-B receptor increases the rats' propensity for developing pulmonary hypertension.

It is well-established that the pulmonary arteries remodel with pulmonary hypertension [1 and the references contained therein], and the remodeling within the lung is well-characterized [2-5, 7]. Characterizing the pathology and, particularly the mechanics of the pulmonary trunk and the proximal, extrapulmonary arteries is less well-documented. McKenzie, et al. [3] have reported on the biochemical and histological response of the pulmonary trunk to hypoxia-induced pulmonary hypertension, and Wilson, et al. [4] described the pathology of monocrotaline-induced pulmonary hypertension in the "major pulmonary arteries." A few research groups, including those from the University of California-San Diego, Northwestern, and Harvard/University of Vermont [6-9], looked at the mechanics of the left pulmonary artery and branches, but none have studied the mechanical properties of the trunk or compared properties of the right and left main arteries.

Test configurations for determining the mechanical properties of vascular tissue are described in Humphrey's 1995 review of the literature [10]. They include biaxial tests, such as cyclic inflation tests and the bubble test, and a simultaneous tension/inflation/torsion test. For this study on the pulmonary

trunk and main arteries, because we are testing only the media and the pulmonary arteries are extremely compliant, we have chosen to use the simpler and more direct bubble test [11].

Hildebrandt et al. [12] first advocated the use of the bubble test for tissue that could be approximated as a membrane. They estimated the deformations at the center as being spherical, and, although the test was biaxial, displacements did not reflect the anisotropy for the different orientations. In research led by Humphrey [13, 14], the bubble test technique was refined to account for the anisotropy of the displacements with loading and consequently results in a two-dimensional strain energy function.

MATERIALS AND METHODS

The rats used for this study were all males of the Long-Evans line, between 57 and 121 days old. The MCT rats were injected subcutaneously with 60 mg/kg at approximately 56 days, and were sacrificed 4 weeks after injection. Knock-out rats were housed in a hypobaric chamber for 3 weeks prior to sacrifice. At the time of sacrifice, each rat was administered a lethal dose (100 mg/kg) of pentobarbital. The complete extrapulmonary arterial system was removed and stored on ice. The lungs of 4 rats (2 Control and 2 MCT) were perfused prior to sacrifice in order to obtain histological verification of the presence or absence of pulmonary hypertension.

The trunk and main arteries were kept refrigerated from the time that they were excised until they were prepared for testing. That time interval was less than 22 hours so that testing could be completed within 24 hours. The left main artery was removed from the trunk, cut longitudinally, and trimmed of any extraneous material, including much of the adventitia, up to the outer elastic lamina. The opened artery was placed with the intimal side up on an O-ring, making sure that the arterial material was wrinkle-free, but not stretched. The specimen and O-ring were placed on the test fixture (Figure 1), aligning the longitudinal direction (the direction of blood flow) with the fluid inlet tube on the fixture. The cap was placed over the specimen and seated with 3 screws. This test fixture was designed especially for the very small pulmonary arteries obtained from these rats, typically 1–2.5 mm in diameter. The O-ring has a 3-mm diameter, and the diameter of the aperture through which the fluid pressurizes the disk-shaped specimen is 2.32 mm.

A schematic of the experimental test setup is shown in Figure 2. Camera 1 was aligned opposite the fluid inlet tube to view deformation of the artery in the circumferential direction. Camera 2 was located 60° and camera 3 120° from camera 1. The pressurizing system, including bellows and tygon tubing was filled with buffered saline solution (or medium), and the specimen placed in a de-ionized (or distilled) water bath heated to 37 °C. Each specimen was manually cycled 5 times to 3.45 kPa (25.9 mm Hg) to precondition the tissue. The computer program automatically acquired vertical images every 0.34 kPa and horizontal images every 1.38 kPa. The tests were typically run up to 17.9 kPa (134 mm Hg, the equivalent of extreme hypertension in the pulmonary artery).

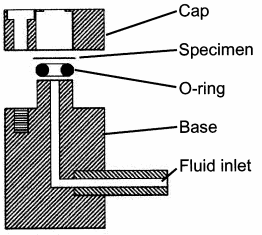

Figure 1. Schematic of the test fixture.

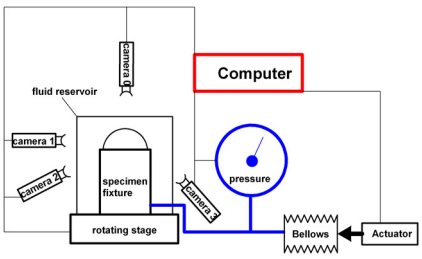

Figure 2. Schematic of the computer-driven test setup.

Upon completion of the test, the specimen was deflated and removed from the fixture. The tissue was microscopically inspected for tears and the thickness was measured with a laser micrometer. As many readings as possible were collected in 30 sec before the tissue desiccated. Values from near the edges or at folds were not recorded. The test procedure was identical for the right main and the trunk, with the exception that a punch was used to trim the trunk specimen to the proper size.

Images at 0° and 90° were used to analyze stress and strain, employing digital image analysis. The approach was to measure the length of the profile l across the top of the bubble at a given pressure; knowing the original length across the flat, uninflated medial artery material, the stretch λ for each orientation could be calculated. The Hencky strain was then calculated from $\varepsilon = \ln(\lambda)$. By assuming that the arterial material was incompressible (constant volume), the thickness of the tissue based on the area of the bubble at each pressure increment could be calculated. Due to the anisotropy of the pulmonary artery, the area of the inflated artery was approximated as the partial surface of a general ellipsoid. The semi-axes of the ellipse could be measured from the side-view images. The thickness value was used to calculate stresses at the top of the bubble. This preliminary analysis uses the solution for stresses in a general ellipsoidal thin shell of homogeneous material, as set forth by Flugge [15].

RESULTS AND DISCUSSION

Figure 3a shows the collective data representing the true stress and true strain for the Control rats (n = 7). Data from the trunk (T), the right main (R), and the left main (L) are shown for the circumferential and longitudinal orientations. A great deal of scatter is observed among this data, as was found by Liu and Fung [9]. The arteries from the Control rats exhibited variations in thicknesses within a test group approached 300 %. One of the greatest challenges in analyzing this data was to determine a representative thickness for each test specimen. We are assured through comparative ultrasonic and histologic measurements that there are large thickness differences from one specimen to another, and each specimen shows variations in thickness over the test area. These thickness differences can be accompanied by corresponding displacement differences. For example, the thinnest of the left main arterial specimens, 2100 and 2101, show the largest stresses. But the right main of 2101, which is also the thinnest of that group, shows stiffening behavior by strains of 0.4–0.6 and stresses that are typical of this group of specimens. Figure 4a and b show vastly different inflation profiles of the two main arteries of

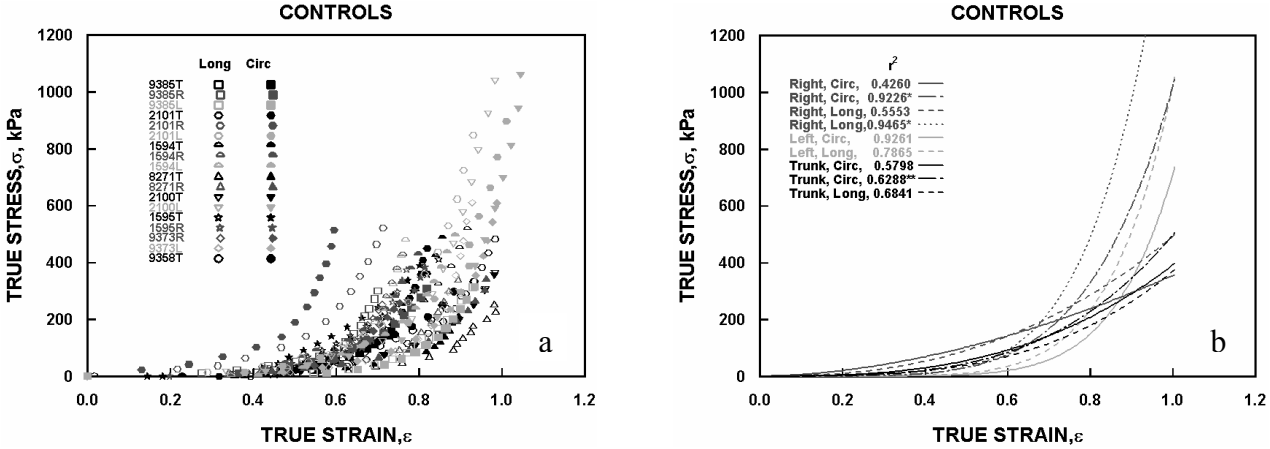

Figure 3. Data showing relation between the true stress and true strain for the Control data. (a) shows the collective data, and (b) shows the fit of each condition to a power-law equation. The r^2 values for each curve fit are found in the figure key, and for r^2 values <0.6 alternative curves are shown with two data sets eliminated. *Specimens 2101 and 8271 were eliminated. **Specimens 2101 and 1595 were eliminated.

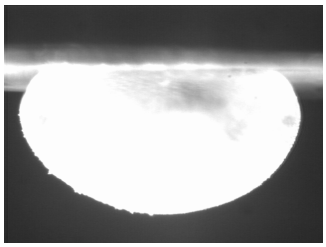
a.
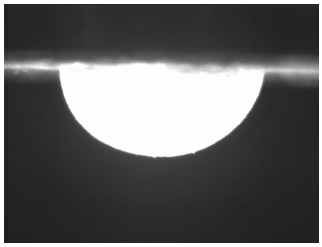
b.

Figure 4. Photographs of specimen 2101 inflated to 16.5 kPa, looking at the circumferential displacements of the (a) left and (b) right main arteries; t_l = 71.1 μm and t_r = 66.0 μm (where t is thickness).

2101 inflated to 16.5 kPa (124 mm Hg), along the 0° orientation. It appears that thickness alone cannot account for the scatter in the data. Nor does it appear that there is a correlation with age, as the data from the oldest specimens (1594 and 1595) fall within the spread of the youngest specimens (2100 and 2101). Rather, it appears that specimen-to-specimen variability, or the intrinsic composition of each specimen, in combination with thickness, governs the stress-strain behavior.

Discerning general trends and behavior among the collective stress-strain data is difficult, so all the data for a particular condition (e.g., all data from the longitudinal, right main artery) were fitted to a single power function of the form $y = Ax^B$. Figure 3b shows the curves fit to the Control data. In cases where the r^2 of the data fell below 0.6, alternative curves are offered where two outlying data sets have been eliminated so as not to skew the data in one direction or another. Figure 5a and b show the stress-strain fitted curves for the MCT rats (n = 5), and for preliminary tests from 2 hypoxic rats, respectively.

In general, the longitudinal orientation of the main arteries showed strain stiffening (where stress rapidly increases with small increases in strain) at lower strains within the population. The circumferential orientation of the right artery demonstrated less strain stiffening than the left artery, which more closely followed the behavior of the longitudinal orientation. And the trunks in both orientations displayed less strain-stiffening behavior than did the main arteries in the range of strains reported for all populations.

The trunk and main arteries (Figure 6b and c, respectively) are bounded by internal and external elastic laminae. The overall thickness of the medial layer of the trunk shown in Figure 6b is about 120

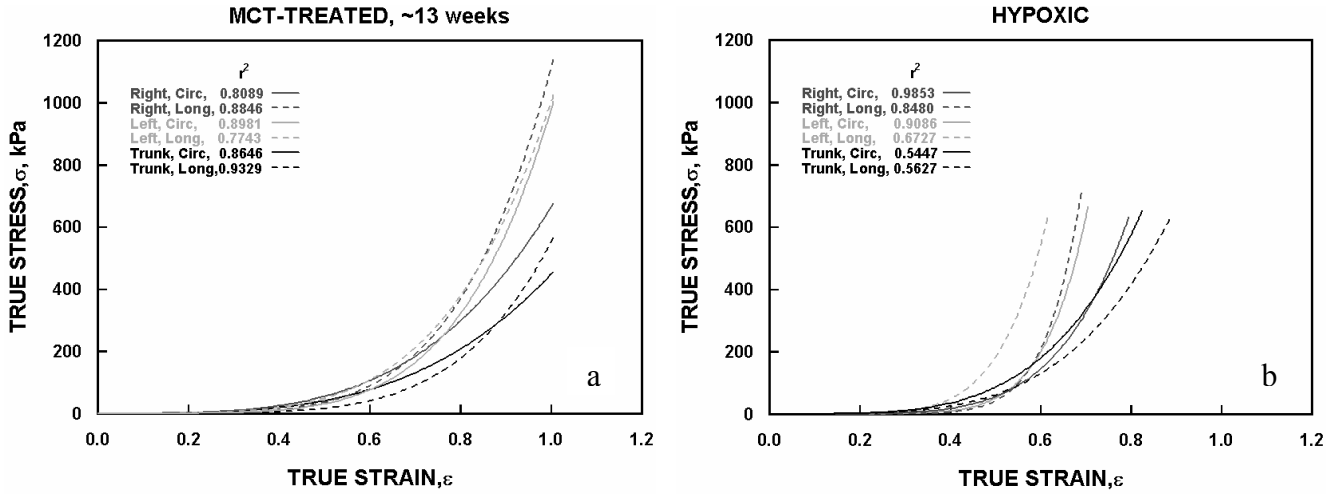

Figure 5. The modeled relationship between the true stress and true strain for the (a) MCT and (b) the Hypoxic data. The r^2 values for each curve fit are found in the figure key.

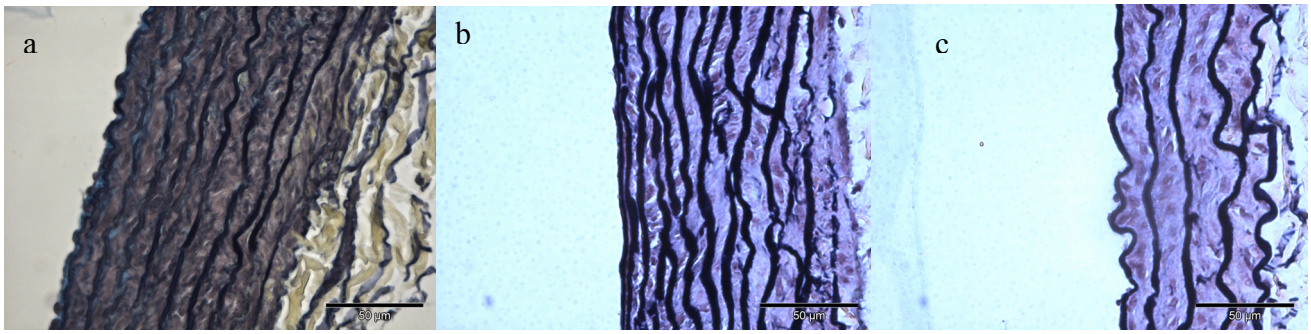

Figure 6. Photomicrographs of (a) the trunk from a Control, (b) the trunk and (c) main artery from a MCT rat stained with pentachrome. Scale bar is 50 µm.

µm, and contains about 12 internal laminae with thicknesses ranging from 2 to 5 µm. The main artery has about 3 internal laminae, and an overall thickness of about 75 µm. The areal fraction of the laminae in these two cases was measured to be 40 and 20 percent for the trunk and main, respectively. The trunk has significantly higher areal fraction (and volume) of elastin, and, therefore, would be expected to exhibit more elastic deformation.

Comparing behaviors among the populations, the main arteries within the Control and MCT populations behaved similarly. Both populations showed tendencies toward strain stiffening at strain of 0.6 to 0.7,whereas indications of strain stiffening were present in the main arteries of the hypoxic popu lation by strains of 0.4 to 0.6. The trunks of the Control population never reached the inflection point indicative of strain stiffening within the load range of these tests. The same is seen in the MCT circumferential curve fit, whereas the inflection in the longitudinal orientation appears to occur near a strain of 0.8. The shallower curves of the hypoxic trunks appears to trend upward, albeit less steeply, at ~0.6.

The subtle differences in the stress-strain properties between the Control population and that of the MCT could lead one to question the degree of pathology engendered by monocrotaline on the proximal arteries. Histological findings comparing lung and arterial specimens from representative Control and MCT rats generally support this implication. Figure 6a and b shows photomicrographs comparing specimens from the trunks of Control and MCT rats. Differences between these extapulmonary media samples are not obvious, and general histological evaluations of lung samples indicated only mild to moderate hypertrophy due to MCT. However, some localized thickening of the extrapolmonary artery samples were noted, so more specimens need to be studied in order to determine characteristic properties of these populations.

In general, the longitudinal orientation showed a greater propensity for strain stiffening than did the circumferential orientation. Physiologically this probably relates to the arteries' need to be responsive circumferentially, but not necessarily longitudinally. There is neither space nor need for the artery to lengthen with each pulse. Those cases where the data do not follow this trend have poor r^2 values for the fit, and we are not prepared to comment on their validity. The stress-strain properties of the trunk and main arteries show more stiffening in the Hypoxic data than in that of the Controls, indicating that remodeling of the media may be occurring; the MCT properties appear similar to the Controls. Also, the relative stiffness of the right and left main arteries switches between the Control and the Hypoxic data.

CONCLUSIONS

We have measured consistent and quantifiable differences in the stress-strain properties between the pulmonary trunk and main arteries, with the main arteries showing more strain stiffening than the

trunk, and there is histological evidence to support this finding. There are quantifiable increases in strain stiffening found in the data from the Hypoxic rats over that observed in the Controls. There is not enough evidence to assert that the stress-strain properties of the proximal pulmonary arteries are affected by the administration of monocrotaline in rats.

ACKNOWLEDGEMENT

The authors thank Kelley Colvin for preparation of the rats and excision of the pulmonary arteries used in this study, and Kendall Waters for his ultrasonic thickness measurements.

REFERENCES

[1] T.K. Jeffery and N.W. Morrell, "Molecular and cellular basis of pulmonary vascular remodeling in pulmonary hypertension," *Prog. Cardiovasc. Dis.*, vol. 45, pp. 173-202, 2002.

[2] B. Meyrick and L. Reid, "Hypoxia-induced structural changes in the media and adventitia of the rat hilar pulmonary artery and their regression," *Am. J. Pathol.*, vol. 100, pp. 151-78, 1980.

[3] J.C. McKenzie, J. Clancy, Jr., and R.M. Klein, "Autoradiographic analysis of cell proliferation and protein synthesis in the pulmonary trunk of rats during the early development of hypoxia-induced pulmonary hypertension," *Blood Vessels*, vol. 21, pp. 80-9, 1984.

[4] D.W. Wilson, H.J. Segall, L.C. Pan, and S.K. Dunston, "Progressive inflammatory and structural changes in the pulmonary vasculature of monocrotaline-treated rats," *Microvasc. Res.*, vol. 38, pp. 57-80, 1989.

[5] P. Davies and L. Reid, "Hypoxic remodeling of the rat pulmonary arterial microcirculation assessed by microdissection," *J. Appl. Physiol.*, vol. 71, pp. 1886-91, 1991.

[6] Y.C. Fung and S.Q. Liu, "Changes of zero-stress state of rat pulmonary arteries in hypoxic hypertension," *J. Appl. Physiol.*, vol. 70, pp. 2455-70, 1991.

[7] D. Langleben, J.L. Szarek, J.T. Coflesky, R.C. Jones, L.M. Reid, and J.N. Evans, "Altered artery mechanics and structure in monocrotaline pulmonary hypertension," *J. Appl. Physiol.*, vol. 65, pp. 2326-31, 1988.

[8] S.Q. Liu, "Alterations in structure of elastic laminae of rat pulmonary arteries in hypoxic hypertension," *J. Appl. Physiol.*, vol. 81, pp. 2147-55, 1996.

[9] S.Q. Liu and Y.C. Fung, "Changes in the structure and mechanical properties of pulmonary arteries of rats exposed to cigarette smoke," *Am. Rev. Respir. Dis.*, vol. 148, pp. 768-77, 1993.

[10] J.D. Humphrey, "Mechanics of the arterial wall: review and directions," *Crit. Rev. Biomed. Eng.*, vol. 23, pp. 1-162, 1995.

[11] E.S. Drexler, A.J. Slifka, J.E. Wright, C.N. McCowan, D.S. Finch, T.P. Quinn, J.D. McColskey, D.D. Ivy, and R. Shandas, "An experimental method for measuring mechanical properties of Rat pulmonary arteries verified with latex," *J. Res. NIST*, vol. 108, pp. 183-191, 2003.

[12] J. Hildebrandt, H. Fukaya, and C.J. Martin, "Stress-strain relations of tissue sheets undergoing uniform two-dimensional stretch," *J. Appl. Physiol.*, vol. 27, pp. 758-62, 1969.

[13] J.D. Humphrey, D.L. Vawter, and R.P. Vito, "Quantification of strains in biaxially tested soft tissues," *J. Biomech*., vol. 20, pp. 59-65, 1987.

[14] F.P.K. Hsu, A.M.C. Liu, J. Downs, D. Rigamonti, and J.D. Humphrey, "A Triplane Video-Based Experimental System for Studying Axisymmetrically Inflated Biomembranes," *IEEE Trans. Biomed. Eng*., vol. 42, p. 442-450, 1995.

[15] W. Flugge, *Stresses in Shells*, New York: Springer-Verlag, 1973.